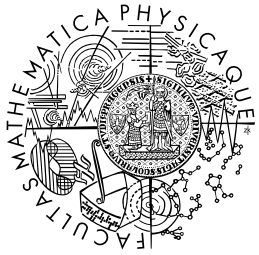

FACULTY
OF MATHEMATICS
AND PHYSICS
Charles University

BACHELOR THESIS

Lea Uhliarová

Time calibration of the ATLAS Tile Calorimeter

Institute of Particle and Nuclear Physics

Supervisor of the bachelor thesis: doc. RNDr. Tomáš Davídek, Ph.D.
Study programme: Physics
Study branch: General physics

Prague 2017

I declare that I carried out this bachelor thesis independently, and only with the cited sources, literature and other professional sources.

I understand that my work relates to the rights and obligations under the Act No. 121/2000 Sb., the Copyright Act, as amended, in particular the fact that the Charles University has the right to conclude a license agreement on the use of this work as a school work pursuant to Section 60 subsection 1 of the Copyright Act.

In ..... date ..... signature of the author

Title: Time calibration of the ATLAS Tile Calorimeter

Author: Lea Uhliarová

Institute: Institute of Particle and Nuclear Physics

Supervisor: doc. RNDr. Tomáš Davídek, Ph.D., Institute of Particle and Nuclear Physics

Abstract:

The ATLAS is one of several particle experiments at the Large Hadron Collider at CERN. Millions of particles are colliding in it every second and it is one of two experiments which have proved the existence of the Higgs boson in 2012. The ATLAS experiment has two main goals. The search for new physics phenomena and precision measurement of the particle interactions.

It consists of a complex system of detectors and read out electronics. The calibration of the whole system is essential for getting correct results and making reasonable conclusions. This thesis is aimed to time calibration of Tile Calorimeter, which is one of calorimeters measuring energy of particles issued from the collision. Time monitoring and correction is performed primarily using laser pulses. In this thesis we described the used laser method which leads to the good time setting.

Keywords: ATLAS, Tile Calorimeter, calibration

Contents

.

Introduction

The ATLAS experiment [1] is the biggest experiment at the LHC (Large Hadron Collider) at CERN. It investigates wide range of physical processes and has two main goals. First goal is to detect new particles that had been previously predicted by theory, especially by Standard Model, but had never been observed before. There is a famous example of particle called the Higgs boson. It was predicted by Robert Brout, François Englert and Peter Higgs in 1964 and its existence was not certified until July 2012, thanks to ATLAS (and CMS) experiment. The second goal of LHC is to study exact characteristics of known particles and their interactions. For example one of the latest published papers presents results of mass measurements of W-boson and another shows results from studies of decaying properties of the Higgs boson.

In 2010, LHC enabled collisions of particles at the energy of 7 TeV. Proton-proton, proton-lead and also lead-lead collisions were taking place in ATLAS. After a pause of two years (beginning in February 2013) for maintenance and upgrades for higher luminosity, it is nowadays possible to collide protons at the total energy of 13 TeV. The attained instantaneous luminosity is $5 \cdot 10^{34}\,\mathrm{cm}^{-2}\mathrm{s}^{-1}$.

1. ATLAS detectors

Focused beams of protons accelerated in LHC enter ATLAS from the two ends and collide inside it. The collision point is surrounded by complex system of detectors weighing all together approximately 7 000 tonnes. The collided bunches of protons give birth to a considerable number of other particles. These particles decay and interact with the matter of detectors. As a result we are able to detect products of these decays and interactions. Those are observed by a set of detectors and sub-detectors. Detectors are arranged radially around the path of protons, respectively inner detector, calorimeters and muon spectrometer. Calorimeters are divided into two main groups: electromagnetic and hadronic calorimeters.

1.1 Inner detector

The inner detector is the closest to the collision point. Paths of charged particles can be observed thanks to ionization of the detector medium. The detector is placed inside the central solenoid which provides magnetic field of 2 T indispensable to the momentum measurement. With the knowledge of paths of the particles and the magnetic field, it is possible to determine momenta of the particles. The inner detector is composed out of three sub-detectors: pixel detector, semiconductor tracker and transition radiation tracker. The radius of the whole detector is 1.15 m.

1.2 Calorimeter

Calorimeters are designed to measure energy and direction of movement of neutral and charged particles. Particles from the proton-proton collision interact with the matter of calorimeters, give birth to other particles during showers (which have electromagnetic and hadronic components), loose energy (ionization, Compton effect, photoelectric effect,etc.) and at the end they are absorbed. As a result, all energy of the particle is deposited in the calorimeters. The measurement of energy is more precise for more energized particles. The relative uncertainty of determined energy is proportional to $\frac{1}{\sqrt{E}}$.

There are two types of calorimeters in ATLAS experiment. Electromagnetic calorimeters, which are made mainly from lead and liquid Argon, are closer to the collision point than the hadronic calorimeters. Electromagnetic calorimeters identify the energy of photons and electrons and hadronic calorimeters those of hadrons, as their name suggests. These two types of calorimeters can detect the energy and the direction of most of the particles from the collision except neutrinos.

1.3 Muon spectrometer

Muons are charged particles which usually penetrate through the inner detector and the calorimeters. They are detected mainly in the muon spectrometer but leave traces also in the inner detector and calorimeters. Muon spectrometer

consists of several different types of chambers which are enfolded in a magnet system. Muons passing through the tubes of spectrometer chambers ionize the gas inside them and thus leave the ions as the signs of its path. In addition, a magnetic field of 4 T is applied to muons thanks to the superconducting toroidal system which is composed by 8 barrels and 2×8 end-cap coils surrounding the muon chambers. Therefore, it is possible to identify and measure the momenta of muons.

1.4 Trigger and data acquisition system

Immense number of proton-proton collisions inside ATLAS detector is the origin of big number of gained data. Approximately $40 \cdot 10^6$ registered cases per second have to be reduced to the maximum of 500 cases because of limited computing possibilities. Complex trigger system [2] chooses the most interesting recorded cases.

The choice of the most interesting data is made by three levels of trigger. Each level reduces considerably the number of data and each makes a more detailed separation than the previous one. As a result, there are just about a few hundred cases per second channelled through data acquisition system to the storage for further analysis.

1.4.1 Level 1 Trigger

Level 1 (L1) Trigger System makes an initial event reduction and reduces the recording rate of 40 MHz to around 100 kHz. Overall, L1 Trigger system has at maximum 2.5 μs for accepting or denying an event. As long as this time can not be exceeded the nominal latency for L1 Trigger was set to 2.0 μs. Most of this time is used for transporting information through cables. The short time for event selection is the reason why L1 Trigger uses reduced granularity data. The main components of decision making process of the L1 Trigger System are:

- L1 Calorimeter Trigger
- L1 Muon Trigger
- Central Trigger Processor.

L1 Calorimeter Trigger handles data from both Liquid Argon Calorimeter and Tile Calorimeter and L1 Muon Trigger those from Muon Spectrometer. Pieces of information from L1 Calorimeter and L1 Muon Trigger are then associated in the Central Trigger Processor and the L1 Trigger makes a final decision.

2. Tile hadronic calorimeter

2.1 Hadronic calorimeter

Hadrons are particles composed from quarks q and antiquarks $\bar{q}$ which are hold together due to the strong interaction. In nature, we observe two types of hadrons, baryons qqq and mesons $q\bar{q}$. To name a few:

- baryons: proton, neutron, Λ^0, Ω
- mesons: pion, kaon, $\rho, \mathrm{B}^0, \eta_\mathrm{c}$.

When a particle enters in the calorimeter, it looses energy as well as interacts with the matter of the detector and launches out showers of secondary particles. Secondary particles interact with the matter of the detector in their turn. Gradually, the energy of daughter particles decrease to a critical value. After the critical value is attained the particle does not loose energy by producing jets any more. It looses energy passively, for example by ionization, bremsstrahlung, etc. Then the process is stopped. It is important for the full detection of the energy of particles that the calorimeter is big enough to absorb all the products from multiple showers which are occurring in it. Therefore, we say that calorimeters are destructive type of detectors. They completely take in particles (except muons and neutrinos) and all their energy. Thus, the thickness of calorimeters has to be several interaction lengths.

In a hadronic calorimeter there may develop two types of showers depending on the entering particle. It can evolve electromagnetic shower or hadronic shower. The source of an electromagnetic shower are neutral pions which decay in the detector and produce two photons. These initiate electromagnetic shower.

Purely hadronic shower can result in wide range of particles:

- high energetic hadrons
- low energetic charged hadrons
- low energetic neutrons
- muons and neutrinos.

The hadronic calorimeter at ATLAS experiment is composed from two main parts, see figure 2.1. There are 3 barrel calorimeters around the beam axis and 2 end-cap calorimeters at the ends. The hadronic end-cap calorimeters are liquid Argon calorimeters and serve as a direct support to electromagnetic end-cap calorimeters. Three barrel calorimeters, between them, form together the Tile Calorimeter in which we are interested and will discuss more into details in the rest of this thesis.

2.2 Composition and construction

Tile Calorimeter (TileCal) [1] is a sampling hadronic calorimeter placed between the electromagnetic calorimeter and the muon detector. TileCal is formed by

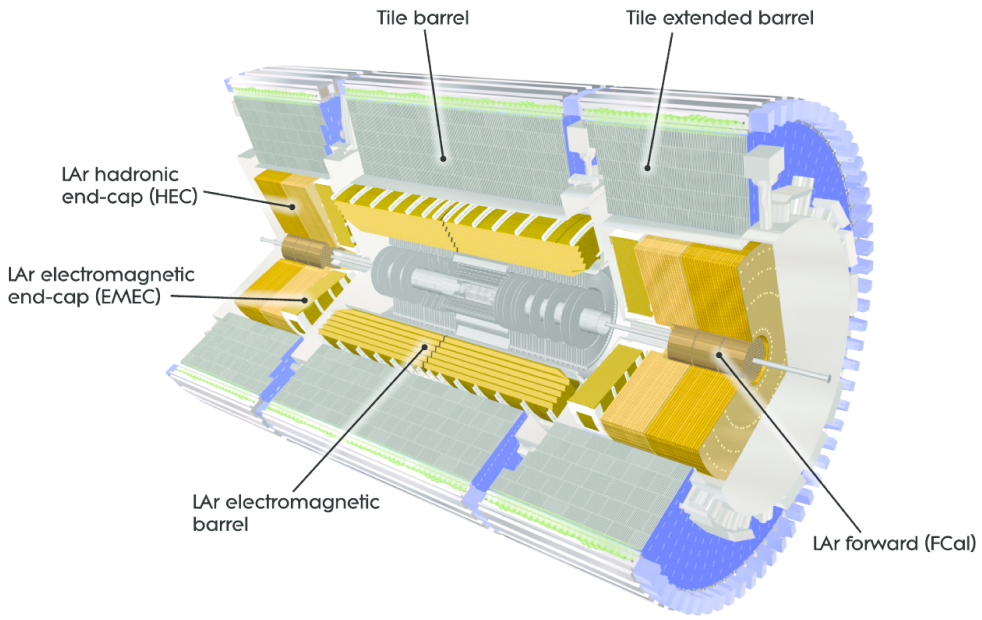

Figure 2.1: The whole ATLAS detector system with highlighted calorimeters, both electromagnetic and hadronic [3].

three barrel calorimeters. Central barrel is 5.6 m long and each of two extended calorimeters is 2.7 m long. The weight of the whole Tile Calorimeter is approximately 2 600 tonnes and it is supported by saddle beams from both sides (parallel to the beam axis). Barrels are arranged along the beam axis covering 360 degrees at the plane perpendicular to the axis. Together with the end-cap hadronic calorimeters TileCal covers almost whole spatial angle 4π. As a result, the missing transverse energy can be determined. Therefore, it is possible to figure out the total transverse energy of non-detectable particles by calorimeters such as neutrinos.

Each barrel itself is a complicated system of tiles, optical fibres, etc. and construction which holds it jointly. The composition of the central barrel calorimeter and the extended calorimeters is almost the same only with little changes in terms of number of components, because extended calorimeters are smaller than the central one.

TileCal is a sandwich type of calorimeter. That means the active layer and the passive layer have to alternate along the path of showers. Absorbing, or passive, layer provides an environment for showers to develop. In TilCal, absorber is made from steel. Active layer is necessary to collect information about the energy of particles passing through the detector. In TileCal, it is realized by plastic scintillation tiles. The sandwich structure of the calorimeter assures good spatial resolution. Scintillator tiles alternating with steel tiles are assembled to modules of barrel calorimeters, see figure 2.2. The central barrel calorimeter is build from 64 modules which are placed around the beam axis. Each one of these modules covers about 0.1 radians in the perpendicular plane to the beam axis.

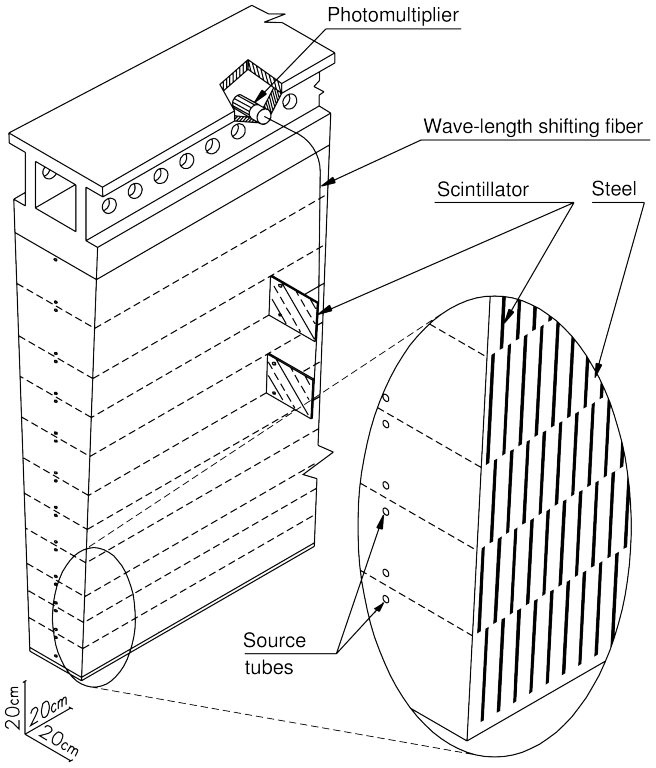

Figure 2.2: Scheme of one TileCal module with its scintillation tiles, steel tiles and read out system [3].

2.3 Read out system

Very important part of the calorimeter is the read out system [4]. Each module (see figure 2.2) of the central barrel is divided in 23 read out cells aligned in three rows (radially), see figure 2.3. On both sides of the module, wavelength-shifting fibres gather the signal from the scintillation tiles. The plastic inside wavelength-shifting optical fibres is doped with a special dye. It absorbs the blue light which is collected from the scintillators and reemits the green light. This mechanism was developed so that the change in the direction of light occurs smoothly. The direction in which the optical fibre reads the signal from scintillators is perpendicular to the direction of sending the light towards photomultipliers. One cell is read out by two photomultipliers, one from each side of the cell. The resultant signal is the sum from both sides of the cell. In order to be protected, optical fibres are grouped in plastic channels leading to photomultipliers located in the girder. Afterwards, the optical signal is converted to the electric signal and sent to the read out electronics.

2.4 Read out electronics and signal processing

As we already mentioned in the previous chapter 1.4, it is inevitable to reduce the data quantity and in order to assure that, there are three levels of trigger along the signal propagation. We described the first level of trigger and we will further examine what happens with the signal from TileCal, until the system obtains information about L1 accept or deny [2].

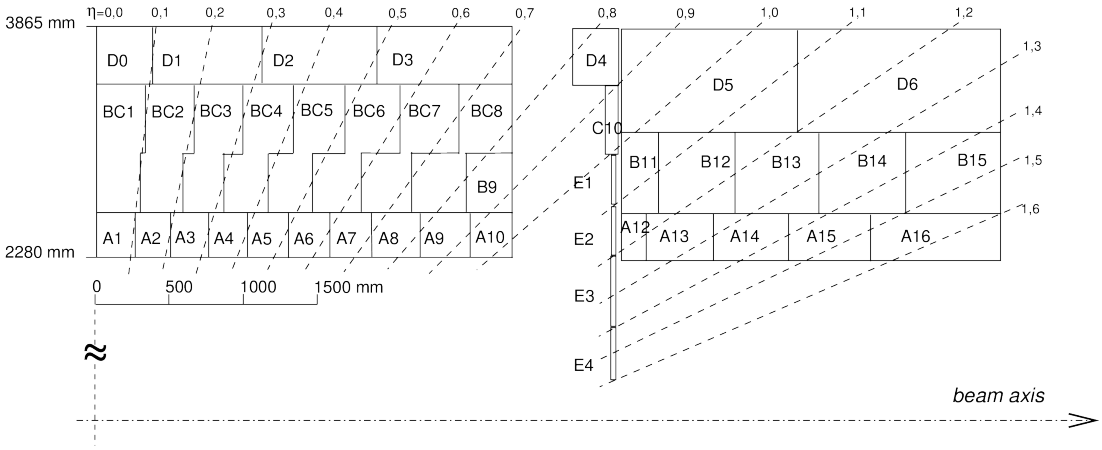

Figure 2.3: Layout of read-out cell organisation. Left part shows half of the central barrel and the right shows the extended barrel [3].

Signal from photomultiplier is pre-processed in 3-in-1 card which has multiple functions. First important function is that it shapes the obtained pulse and divides it into two branches, called high gain and low gain. It amplifies the signal for the high gain in ratio 64:1, comparing to the low gain, in order to cover the large dynamic range issued from the fact that particles inside the detector possess very different energies. At this stage, it is possible to recognise muon signal from noise which are both small. The second role of 3-in-1 card important for this work is sending analogue signal to L1 Trigger.

In each gain branch (high and low), there is an analogue-to-digital converter (ADC) equipped with a memory. Both ADCs are sampling the shaped pulse received from photomultipliers. They read one signal each 25 ns and are able to store them in buffers up to several μs. When information concerning L1 Trigger accept of an event comes, the 7 corresponding values of the pulse are read from both ADC memories. These two sequences are compared and one of them, usually the high gain sequence, is chosen. Sequence from the low gain is preferred over high gain if the high gain signal is saturated, which means that at least one of 7 values is 1023 counts high. This number is given by the nature of ADC counter, which is a 10-bit converter. High and low gain branches from 6 channels are drawn together in one hardware board called digitizer. From digitizer, the digitalized signal is passed out of TileCal. It is submitted to read out drivers (ROD) and next levels of trigger.

ROD performs reconstructing of the pulse and some of its parameters. In the figure 2.4, we can see parameters which are detected by ROD:

- amplitude A - the height of the peak of reconstructed pulse
- time phase t_0 - the position of the peak in time.

As the shape of the reconstructed pulse is always the same (thanks to shaping in 3-in-1 card), it is possible to determine energy from the amplitude A. There is no need to integrate the surface below the curve, it is sufficient to measure the height of its peak A. We will specify the significance of t_0 in the chapter 4.

The algorithm used in ROD is called Optimal Filtering. This approach is simpler and faster than other possible fitting methods. In the ROD, Optimal

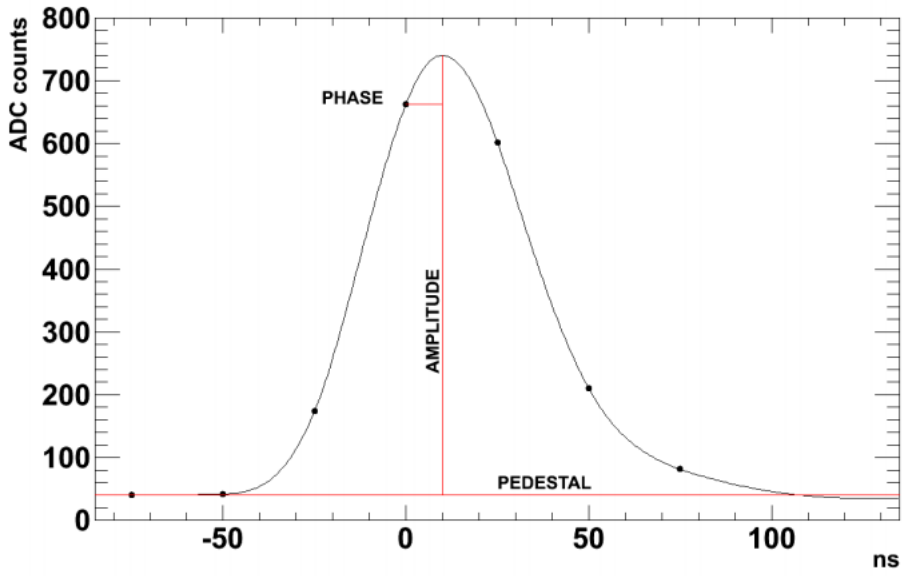

Figure 2.4: Fit of the pulse by ROD [5].

Filtering is used without iterations in order to reconstruct channel energy in the fastest way possible. Finally, the picked-up events are forwarded to data acquisition and storage system for further offline analysis.

3. Calibration

Calibration of the TileCal read out systems is inevitable for precise signal registration. The relative changes between cells have to be minimized and the whole system has to be monitored in order to recognize any non-linear response. It is possible to correct such discrepancies but we need to obtain information about them. That is assured by 4 calibration systems (see figure 3.1) at different levels of the TileCal read out system [6]. For the adjustment of the electromagnetic scale is used following formula:

$$E = A \cdot C_{Cs} \cdot C_{CIS} \cdot C_{las} \cdot C_{TB}, \tag{3.1}$$

where A is amplitude of the signal, C_{TB} is a constant for converting pC to GeV. C_{TB} constant was established during TileCal test beam [7]. The rest of constants used in 3.1 will be explained in the sections below.

- **radioactive source**

  ^{137}Cs is gamma radioactive source used to calibrate tile optical parts and photomultipliers. During special Caesium runs it is injected to the steel tubes inside TileCal modules and passes through every scintillation tile. The result of Caesium calibration is the calibration constant C_{Cs} which is implemented to the system later. Caesium calibration is taken about once in two months and it leads to the precision of the optical systems better than 0.3 %.

- **laser**

  A few times a week, laser is sent to all photomultipliers at once through specific optical fibres during a time dedicated to special laser runs [8]. The laser beam has good properties to simulate real physics signal and to saturate all read out channels. The outcome of laser runs is calibration constant C_{las}. The C_{las} constant serves for good adjustment of photomultiplier tube gains and provides a calibration aimed on a precise energy read out. In addition, laser runs help to discover non-linearities in the photomultiplier response.

  Laser signal is also used for time calibration [8], [9]. For this purpose, the laser is sent to the TileCal in so called empty orbits. That is a several μs gap between two successive collisions. Therefore, laser beam for monitoring accuracy of time set of TileCal is emitted during periods of gathering physics data and the response of TileCal to laser can be associated and compared with data from physics runs.

- **charge injection system (CIS)**

  Injection of precisely defined amount of charge is followed by detection of the electronic response of front-end electronics. CIS is used for correct energy reconstruction and for monitoring of read out system and its linearity. The final constant is very stable and the precision of CIS calibration is approximately 0.7 %.

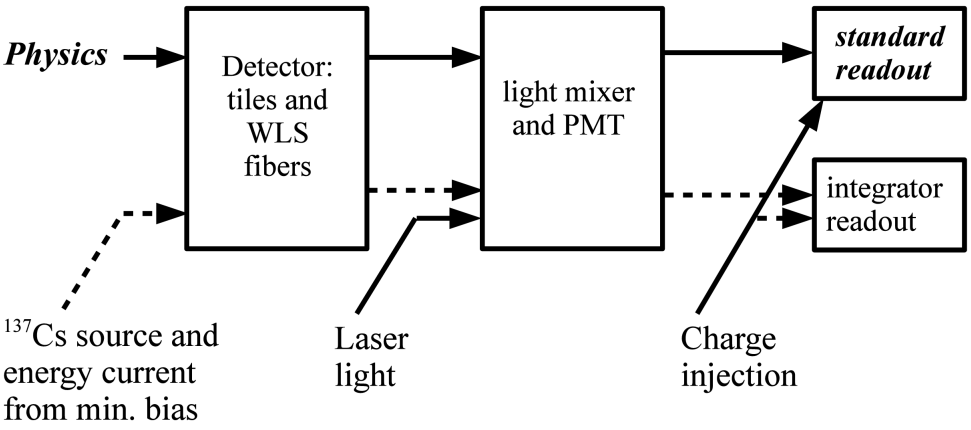

Figure 3.1: Calibration systems of TileCal [3].

- **minimum bias (MB) system**

  Soft parton collisions or minimum bias events are very common in collisions of two high energy proton clusters from LHC. In MB events originates considerable amount of background signal. Minimum bias system uses integrators to integrate the current, acquired from photomultipliers, over time (in range of milliseconds). The integrated current is subsequently used for supervising channel stability. Furthermore, the luminosity can be determined from the integrated current, considering that these two are proportional.

4. Time calibration

Optimal Filtering (OF) method is an algorithm capable of reconstructing amplitude A and therefore energy deposited in a calorimeter cell. OF was chosen among other approaches because it works with good resolution and needs relatively short processing time. Nevertheless, the energy reconstruction depends on time phase of the incoming signal. If the phase is not well established the reconstructed amplitude and energy values are smaller than the real ones. It is possible to use parabolic correction (see figure 4.1) for adjusting reconstructed amplitude but that can cause redundant uncertainty for greater differences in phase. In order to detect the right phase of the signal, TileCal uses time calibration [8]. Besides the time phase establishment, time calibration is useful for:

- elimination of abundant energy depositions from cosmic particles, non-collision background, etc.
- time-of-flight measurement, used to potential finding of massive exotic particles.

The aim of the time calibration is to set the local time of incoming signal to $t_0 = 0$ for each channel. In other terms, the reconstructed peak (amplitude A) should manifest itself at local time $t_0 = 0$. The absolute time calibration of TileCal is performed by cosmic particles, splash events and physics jets themselves. Splash events provide the highest precision of the time calibration, up to 0.6 ns in one module. Process called splash takes place when one proton bunch collides with a closed collimator and this results in millions of high energetic particles, together leaving in calorimeters energy of an order of TeV. Advantage of calibration by splash events and physics jets is high statistics.

The absolute calibration is set before physics runs [9]. For precise energy data interpretation it is essential to monitor time calibration also during physics runs and report if any changes are observed. The monitoring part is maintained by laser emitted in empty orbits (see chapter 3). From each emission of laser in empty orbit we have in our disposition histograms for every channel.

4.1 Timing jumps

Each digitizer can handle up to 6 read out channels. These 6 channels have tendency to behave in the same manner. If there is need for correcting previously established calibration constant, we observe timing jumps in histograms of reconstructed time [8].

My supervisor wrote a software utility for easier analysis of histograms for time calibration. It filtrates standard behaving channels, like in the figure 4.2, from the ones with jumps (figure 4.3) or other deviations from standard. It chooses only the cases where a change in time is greater than 3 ns. For memory reasons, it is not possible to correct every little jump, so the reasonable limit of 3 ns was chosen. Thus, low disturb signals will not be further taken into account.

For each run with abnormal response in any channel, the macro generates a file, listing all the deflections. The objective of this thesis was to go through

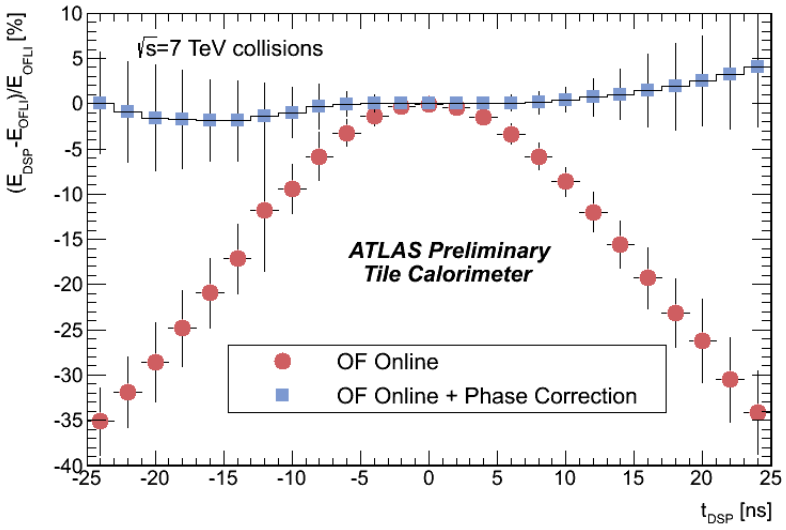

Figure 4.1: Reconstructed energy based on Optimal Filtering algorithm [10].

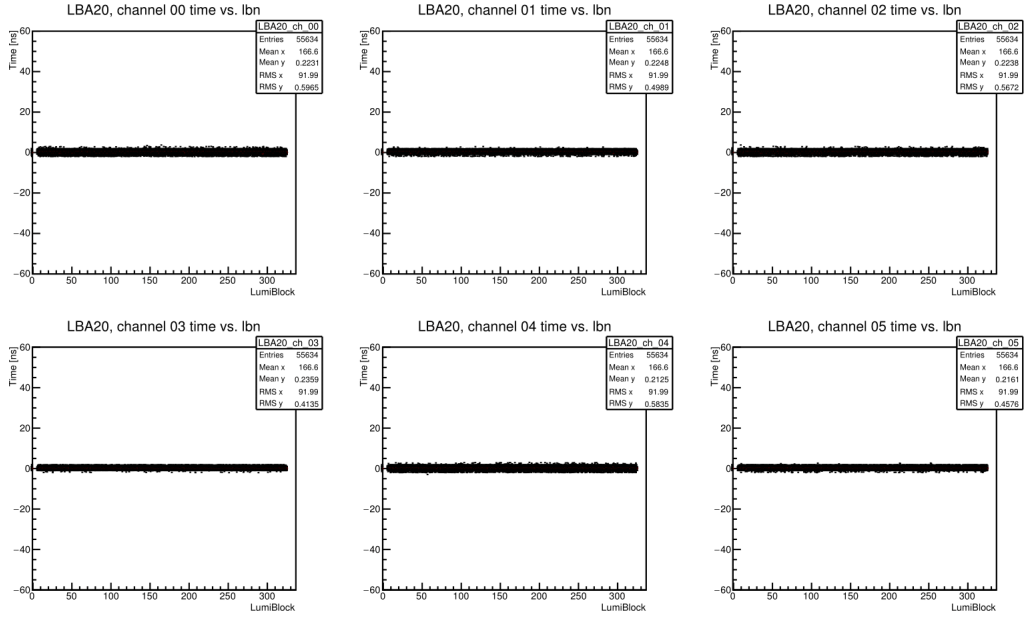

Figure 4.2: Standard channels.

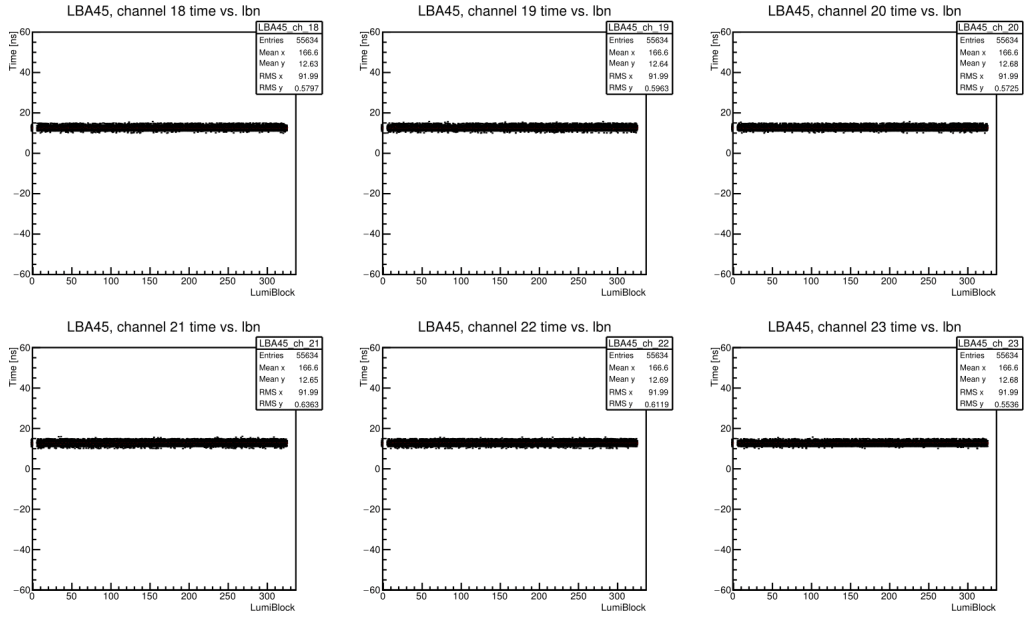

Figure 4.3: Channels with 12.7 ns jump during whole run.

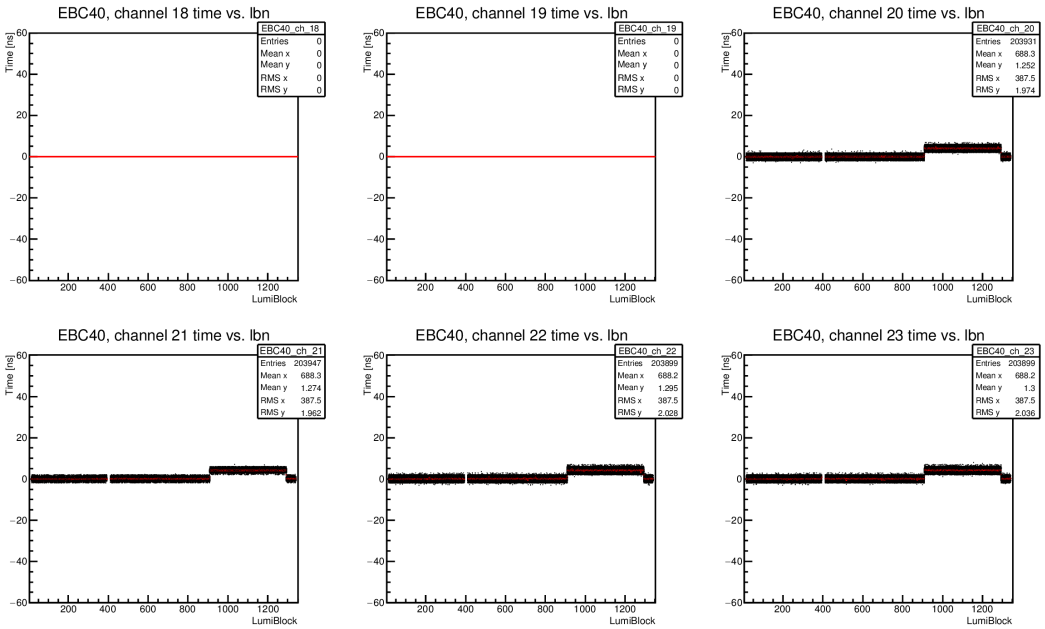

Figure 4.4: Channels with 4.2 ns jump which begins and ends in the same run.

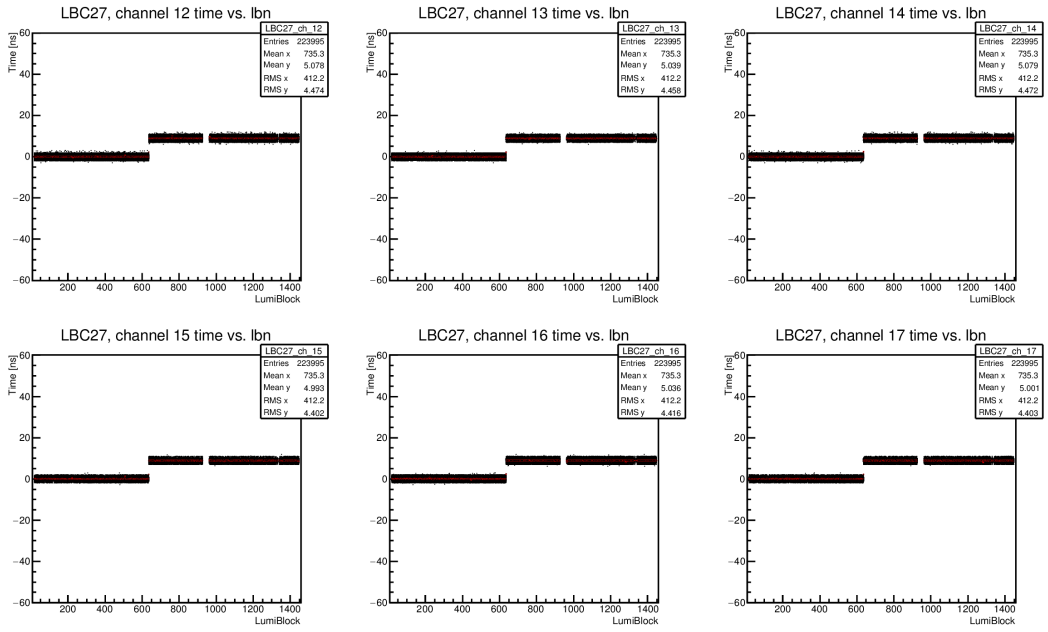

Figure 4.5: Channels with 8.9 ns jump beginning later in the run.

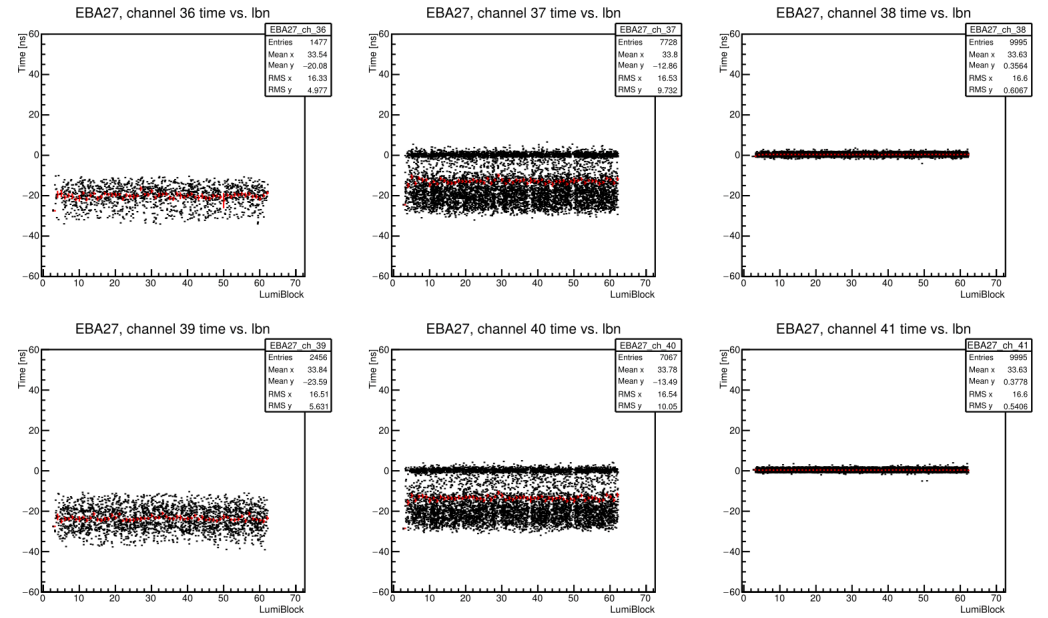

Figure 4.6: Channels with large spread.

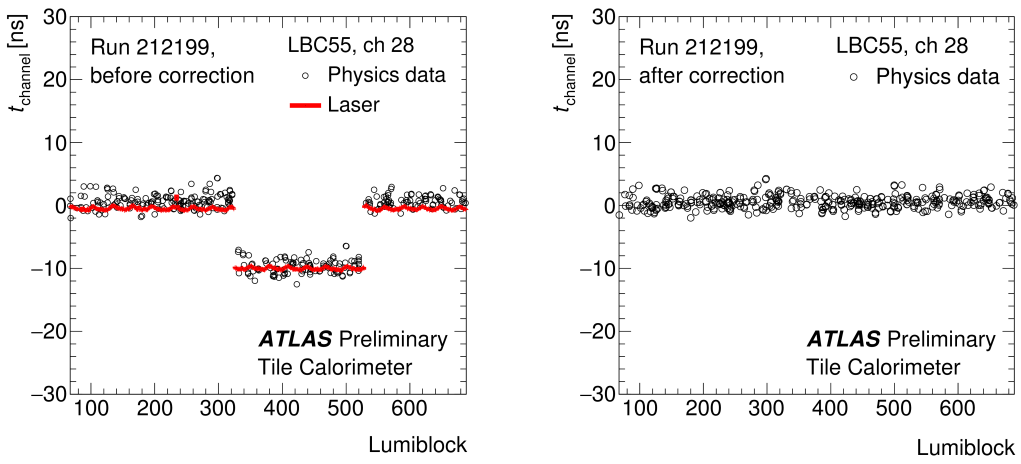

Figure 4.7: Histograms from laser and physics data before and after correction [11].

all listings from year 2016 (Run-2) manually, check them and investigate unusual cases. One part consisted from controlling if the macro worked well, if the listed jumps were present in histograms and if the timing jumps were also visible in physical runs. The second part was dedicated to studying special cases, when it was not clear what was happening from the file produced by macro.

In the following, we will describe the most exemplar cases to acquire an overview. In order to have a good reference we will at first look at the figure 4.2. In this figure, as in any other, there are 6 histograms. Each histogram corresponds to one channel from 6 belonging to the same digitizer hardware board. X-axis is displayed in time units called LumiBlocks. A LumiBlock is the smallest unit in which we can change the time constant. The y-axis corresponds to reconstructed time in the channel. The figure 4.2 is an example of the normal situation. There is no need for correction, the energy is read out in local time $t_0 = 0$.

Contrarily, the figure 4.3 is a typical situation of timing jumps. We can identify a timing jump of 12.7 ns. It happens in the same manner in all displayed channels.

There are essentially three different types of timing jumps:

- jump occuring during the whole run (figure 4.3)
- timing jump beginning and also ending in the same run (figure 4.4)
- the one beginning in the shown run but not ending in it (figure 4.5), or vice versa.

In the figure 4.4 we can observe, that the jump is taking place only in four channels from six. There is no laser signal recorded in two other channels, namely in channels 18 and 19 from module EBC40. These channels are empty because of construction reasons. In the course of analysis of laser signal it is sometimes important to check a complete listing of empty channels to avoid misinterpretation.

The complication brought into by timing jumps is easily solvable. It just needs some time to use a software and to study it. For rectifying a timing jump, it is inevitable to find out the run and the LumiBlock when it begun and analogously, the run and the LumiBlock when it was over. At that point, it is possible to determine time correction constant and upload it to database for all 6 channel at once.

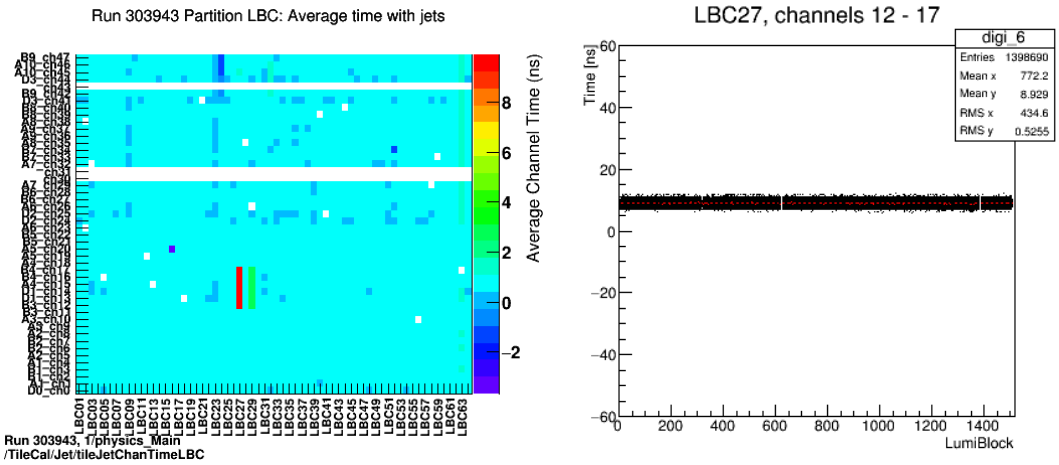

Figure 4.8: Record of time of incoming signal from physics run (on the left side) and correspondent laser histogram (on the right side). Timing jump in module LBC27 in the channels 12 - 17 is shown in red in the figure from physics run.

We can observe the effect of the correction of timing jump in the figure 4.7.

Besides timing jumps we came across special cases. One of them is displayed in the figure 4.6. We observe a large spread of signal in several channels and the spread obviously dominates over timing jumps. As it happens only in a few channels from six, we can assume that there is a problem in those exact channels and not in the read out electronics which is processing them all. In the large spread cases, there is need to blind the physics data from that channel in the time of signal diffusion. If an uncontrollable spread continues for a longer time, the channel is blinded, or masked forever.

4.2 Physics data

While studying the timing jumps, we also checked and confirmed that timing jumps we saw in laser histograms were visible in physics run, too. An example is shown in the figure 4.8. Sometimes, the laser histogram was not available for a period of time and it was necessary to determine if the timing jumps from the precedent run continued. In these cases we examined specific jumps in the monitoring histograms from physics runs. For example, for the bitmap 4.9 we had not any correspondent histogram from laser in our disposition. Still, timing jumps are clearly distinguishable in physics run.

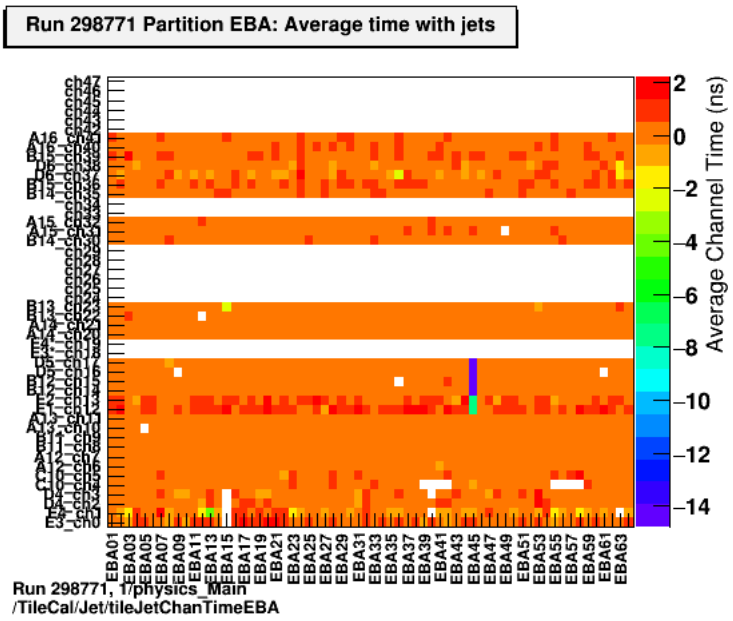

Figure 4.9: Physics run without information from laser. Timing jump in module EBA45 in the channels 12 - 17 is clearly present (shown in blue colour).

Conclusion

We performed monitoring and correction of time setting in the Tile Calorimeter. We used software aimed to the detection of timing jumps in laser histograms and we confirmed its accuracy by comparing histograms with its results. Afterwards, we devoted ourselves to the study of notable cases. It was necessary to locate oddly behaving channels, compare their responses in consequent runs and opt for a solution for each particular case. Except laser histograms, we also scrutinized physics data as we showed in the chapter 4.

All together, we used two main methods to resolve displayed deflections. In case of timing jumps, we furnished a list containing a summary of all channels with timing jumps in observed runs, their values and their precise durations. Correcting timing jumps consists of inserting corresponding time constants to database. In special cases, when it was needed, we adviced to mask the exact channels. Depending on the situation, it was important to mask both physics and laser data or only the laser data.

To conclude, we successfully achieved the original aim of this thesis, which was the detection of timing jumps in the Tile Calorimeter and their correction. Our results were send to CERN, uploaded to the database and they are currently used in data reprocessing. This should improve the time settings and time stability in TileCal in 2016 data.

Bibliography

[1] ATLAS Collaboration. The ATLAS experiment at the cern large hadron collider. *Journal of Instrumentation*, 3:S08003, 2008.

[2] G. Usai. ATLAS tile calorimeter electronics and future upgrades. *Journal of Instrumentation*, 10(4):C04026, 2015.

[3] ATLAS Collaboration. `https://twiki.cern.ch/twiki/bin/view/AtlasPublic/PublishedTilecalFigures`, 2008.

[4] ATLAS Collaboration. The optical instrumentation of the ATLAS tile calorimeter. *Journal of Instrumentation*, 8(1):P01005, 2013.

[5] ATLAS Collaboration. `https://twiki.cern.ch/twiki/bin/viewauth/Atlas/TileTimingCalibration`, 2012.

[6] ATLAS Collaboration. Readiness of the ATLAS tile calorimeter for lhc collisions. *Eur.Phys.J.C70:1193-1236*, 2010.

[7] ATLAS Collaboration. Testbeam studies of production modules of the ATLAS tile calorimeter. *Nuclear Instruments and Methods in Physics Research Section A: Accelerators, Spectrometers, Detectors and Associated Equipment*, 606(3):362–394, 2009.

[8] ATLAS Collaboration. The laser calibration of the ATLAS tile calorimeter during the lhc run 1. *Journal of Instrumentation*, 11(10):T10005, 2016.

[9] Tomáš Davídek. Instrumentace a kalibrace hadronového kalorimetru ATLAS Tilecal. habilitation thesis, Charles University in Prague, 2013.

[10] ATLAS Collaboration. `https://twiki.cern.ch/twiki/bin/view/AtlasPublic/ApprovedPlotsTileSignalReconstruction`.

[11] ATLAS Collaboration. `https://twiki.cern.ch/twiki/bin/view/AtlasPublic/TileCaloPublicResultsTiming`.

List of Figures